IEEE Access
Multidisciplinary | Rapid Review | Open Access Journal

Received May 7, 2021, accepted June 1, 2021, date of publication June 7, 2021, date of current version June 14, 2021.

Digital Object Identifier 10.1109/ACCESS.2021.3087123

An Autonomous Frequency Reconfigurable Antenna Using Slotline Open-Loop Resonators

GERIKI POLAIAH, (Student Member, IEEE), KRISHNAMOORTHY KANDASAMY, (Member, IEEE), AND MURALIDHAR KULKARNI, (Senior Member, IEEE)

Department of Electronics and Communication Engineering, National Institute of Technology Karnataka, Surathkal 575025, India

Corresponding author: Geriki Polaiah (polaiahgeriki@gmail.com)

This work was supported by the National Institute of Technology Karnataka, Surathkal, India.

ABSTRACT This paper presents a slotline open-loop resonators based frequency reconfigurable antenna with autonomous switching of frequency bands. The dual-port slot antenna is designed to operate at 2.1 GHz when excited at port-1, and when port-2 is excited, the antenna can be reconfigured to operate at 2.85 GHz and 5.52 GHz, respectively. Port-1 is used to receive the control signal, which is converted to a DC signal using a rectifier. The rectified control signal is used to switch the operating frequency bands of the port-2. The proposed antenna configuration gives the flexibility of remote/wireless control of the operating frequency. The antenna prototype is fabricated and measured for observing the frequency switching at port-2. The measured results show that the antenna has been effectively switched from lower band frequency (2.8 GHz) to upper band frequency (5.41 GHz) when the PIN diode is ON. The proposed antenna in its final configuration can be potentially suitable for transmitter reconfigurable antenna without the need for external DC bias voltage.

INDEX TERMS Dual-port antenna, frequency reconfiguration, power harvesting, rectifying circuit, slotline open-loop resonators.

I. INTRODUCTION

Frequency reconfigurable antennas have received much attention in the past years due to their selection of multiband operating frequencies and prominent features for effectively utilizing the spectrum. Many mobile communication systems have often used slot antennas because they possess low profile, the possibility of independent frequency tuning, and impedance bandwidth adjustment. In recent years, with the rapid development of communication and power electronics, autonomous frequency reconfigurable antennas have attracted much attention in wireless communication applications because of their unique properties of multiple services in a single antenna without the need for multiple antennas and external DC bias voltage. This type of antennas provides wide tunable impedance bandwidth obtainable without degrading the antenna gain, reflection coefficient, and radiation pattern [1]–[4]. Recently, the frequency reconfigurable antennas in various topologies of slotline with branch edge [5], composite right/left hand (CRLH) transmission line [6], [7], geometrical slots excited by feed line [8], [9], bow-tie microstrip [10], [11], Quasi-Yagi dipole [12], [13], wideband/dual-band microstrip patch [14]–[16], half annular ring slot [17], metamaterial inspired [18], and tunable slot [19], are proposed. In addition to this, frequency reconfigurable antennas with different radiating structures such as rectangular loops with partial patch [20], circular patch [21], monopole configuration [22], quadrifilar helix [23], loop antenna with independent tuning [24], grounded asymmetric CPW fed planar [25], U-shaped monopole radiator [26], and substrate integrated waveguide based reconfigurable antenna [27] are reported. In the antennas mentioned above, a PIN diode/varactor diode is inserted on the specified slots for the effective controlling of frequency bands because they possess low threshold voltage and flexible mounting configuration. An external DC bias voltage and capacitors/inductors for isolating the RF/DC power are essential to operate the aforementioned antennas for frequency reconfiguration. In [23], the adaptive frequency operation is mechanically switched, which changes the

The associate editor coordinating the review of this manuscript and approving it for publication was Diego Masotti.

antenna's electrical length. An autonomous reconfigurable microstrip patch antenna is reported in [28] for frequency switching from 1.2 GHz to 1.5 GHz. Here, the power splitter and bandpass filter are additionally connected to separate the desired frequency band which can be used for the generation of DC control signal. The modern wireless communication system demands efficient autonomous frequency switching reconfigurable multi-band antennas with reduced size and low loss RF circuitry/devices. In the proposed work, a simple configuration of the dual-port antenna using slotline open-loop resonators is designed for frequency reconfiguration (port-2) and the generation of DC control signal (port-1). The required DC biasing voltage of 0.67V (measured using a digital multimeter) for the actuation of the PIN diode is directly received from the connected rectifying circuit at port-1 of the frequency reconfigurable antenna. The antenna resonance frequencies at port-2 are adaptively changed by controlling the diode ON or OFF condition with frequency switching capabilities.

In this work, an autonomously controlled frequency reconfigurable antenna using slotline open-loop resonators can be used at the desired frequency in Universal Mobile Telecommunications System (UMTS) and Industrial–Scientific–Medical (ISM) bands without requiring an external DC control is proposed. The rectifier is connected at port-1 of the antenna for the conversion of RF power to DC voltage, and port-2 is for the frequency switching operation. By controlling the ON or OFF state of the PIN diode on the antenna ground plane and connected the rectified output voltage internally, the proposed antenna for autonomous frequency reconfiguration can operate either in a similar frequency band or in their corresponding bands with independent control.

II. AUTONOMOUS FREQUENCY RECONFIGURABLE ANTENNA

The schematic diagram of the proposed autonomous frequency reconfigurable antenna that does not require an external DC control signal is shown in Fig.1. The proposed antenna configuration is composed of a frequency reconfigurable antenna for receiving the RF power and rectifying circuit for the generation of the required control signal to turn ON the PIN diode for adaptive frequency switching. The turn ON voltage of the PIN diode (0.67V) is directly received from the output of the rectifying circuit. The antenna is designed to operate at 2.1 GHz when excited at port-1, and when port-2 is excited, the antenna can be reconfigured to operate at 2.85 GHz and 5.52 GHz, respectively. Port-1 is used to receive the control signal, which is converted to a DC signal using a rectifier. The rectified control signal is used to switch the operating frequency bands of the port-2. If the antenna receiving signal is at the input of rectifying circuit (at port-1), an RF power is provided to the circuit and converted to a positive DC voltage proportional to the antenna received power. If the RF input power is large enough, the output voltage of the rectifying circuit is reached to diode turn

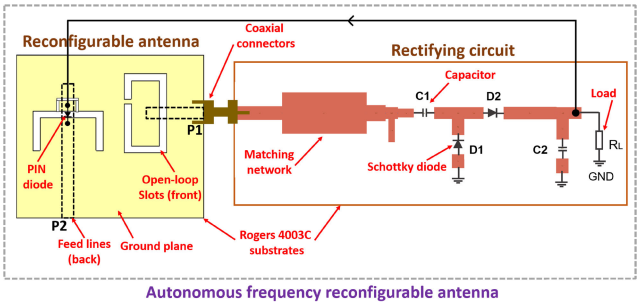

FIGURE 1. Schematic diagram of the proposed autonomous frequency reconfigurable antenna.

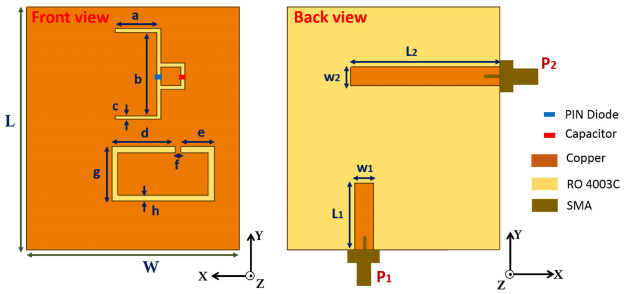

FIGURE 2. Geometry and dimensions of the frequency reconfigurable antenna (L = 40 mm, W = 35 mm, a = 7.6 mm, b = 15 mm, c = 0.6 mm, d = 10.5 mm, e = 5.5 mm, f = 1 mm, g = 9 mm, h = 1 mm, L1 = 11 mm, L2 = 24.5 mm, w1 = w2 =3.1 mm).

ON voltage then the antenna is reconfigured to switching frequency of 5.52 GHz. When the generated DC control voltage is not sufficient to actuate the PIN diode, the antenna is adaptively reconfigured back to its initial operating frequency of 2.85 GHz. The design details and results analysis of frequency reconfigurable antenna and rectifying circuit are discussed in the next subsections.

A. FREQUENCY RECONFIGURABLE ANTENNA

The frequency reconfigurable antenna is designed on a 1.52 mm thickness Rogers 4003C substrate ($\epsilon_r = 3.3$ and $\tan\delta = 0.0027$) in CST Microwave Studio. The geometry and dimension of the frequency reconfigurable antenna are shown in Fig. 2. The antenna has two ports out of which one port is for transferring the RF power to the rectifying circuit for the generation of DC control signal and the second port is used as transmit/receive of RF power. The antenna is designed to operate at 2.1 GHz when excited at port-1, and when port-2 is excited, the antenna can be reconfigured to operate at 2.85 GHz and 5.52 GHz, respectively. An open-loop C-shape and rectangular slots are etched out on the substrate's top side (ground plane). The bottom side is composed of two 50Ω feed lines with optimized lengths to excite the proposed slots for the desired frequencies. The resonance frequency is primarily depending on the loop length, width, and separation distance of the slotline resonator [29]. The resonance frequency is decreased while increasing the loop length, whereas the frequency increases when increasing the separation distance. The reason is that variation in separation distance

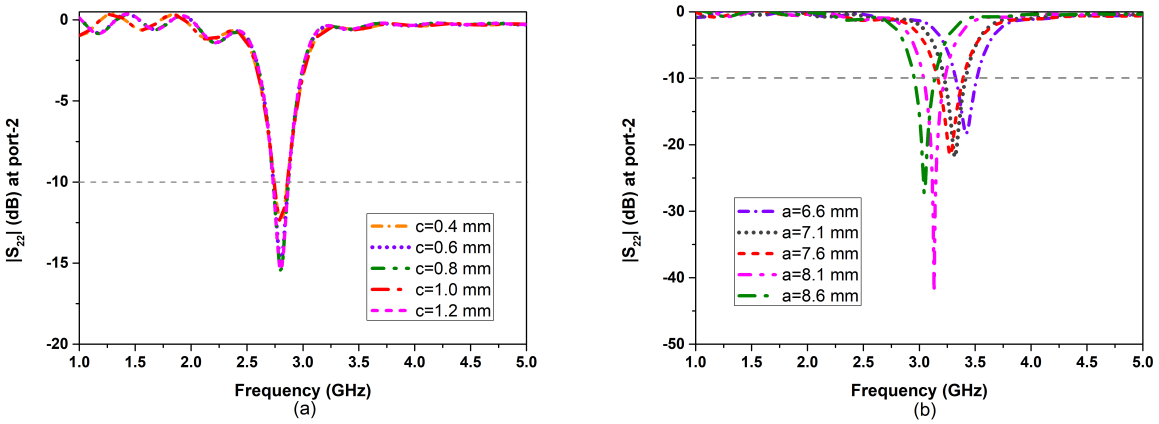

FIGURE 3. Parametric analysis on the resonant frequency bands at port-2 (a) varying the parameter 'c' (b) varying the parameter 'a.'

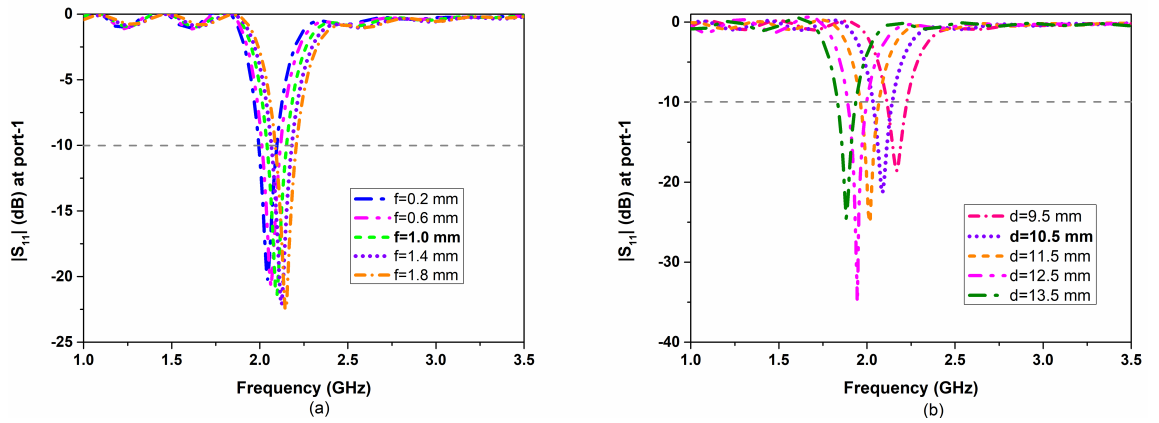

FIGURE 4. Parametric analysis on the resonant frequency bands at port-1 (a) varying the parameter 'f' (b) varying the parameter 'd.'

results change in characteristic impedance (Z_0) and slotted open-loop length simultaneously. In general, the open-loop resonators have maximum electric field density at the side of an open-gap and maximum magnetic field density distributed at the opposite side of the open-gap [30]. Various coupling mechanisms exist between the consecutive open-loop resonators, namely electric, magnetic, and mixed couplings. In this work, we have designed two different single open-loop slotted resonators excited by feed lines for the adaptive reconfiguration of resonance frequencies. The expected first operating frequency of 2.1 GHz (UMTS) at port-1 is obtained by optimizing the total electrical length ($2d+2g+2e+f$), width (h), separation distance (f) of the rectangular slotted open loop, and dimension (L_1,w_1) of the corresponding feed line. The second band frequency of 2.85 GHz (WiMAX) at port-2 is achieved by etching the C-shaped open-loop slot with optimized dimensions and adjust the length/width (L_2,w_2) of the designated feed line.

A PIN diode is inserted exactly at the middle of the C-shaped slot according to the feed line's dimension for frequency reconfiguration. When the diode is ON, the frequency is changing from 2.85 GHz to 5.52 GHz with a large separation of more than 2 GHz at port-2 without altering the first band frequency at port-1. Simulation and measurement results of the frequency reconfigurable antenna are analyzed for reflection coefficient, transmission coefficient, surface current, and radiation patterns. The capacitor, biasing pad, and PIN diode are modeled accurately at the time electromagnetic simulations are performed in CST Microwave Studio. The PIN diode is inserted on the open-loop slot (corresponding at port-2) for frequency reconfiguration without changing the resonance frequency at port-1. The parametric analysis on the resonant frequency bands at port-1 and port-2 is performed by varying the length and width of resonator slots. The change of resonant frequency by varying the parameters 'c' and 'a' on the C-shaped resonator slot is shown in Fig. 3. It is to be observed from Fig. 3(a), the variation of parameter 'c' (slot width) results in no change in resonant frequency. However, as shown in Fig. 3(b), the resonant frequency is slightly shifted to a lower frequency side when the parameter value 'a' (slot length) is increased. The change of resonant frequency by varying the parameters 'f' and

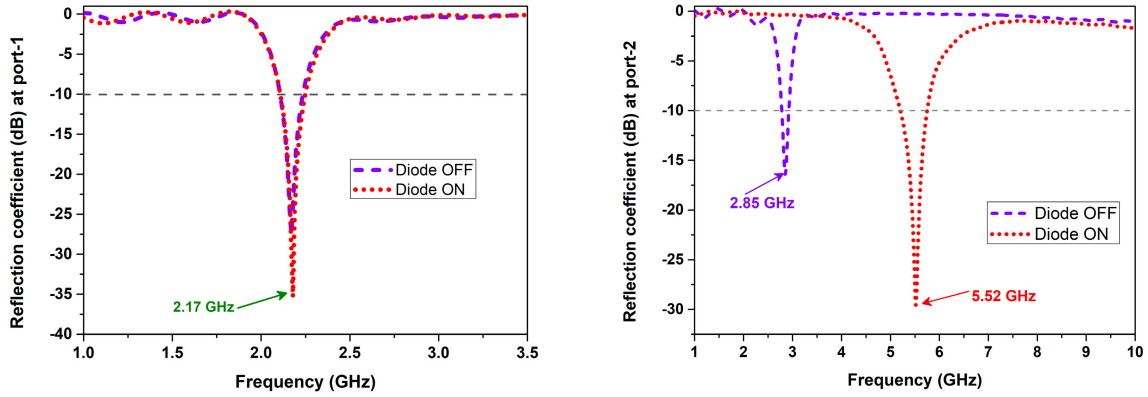

FIGURE 5. Simulation results of magnitude of reflection coefficient versus frequency of the frequency reconfigurable antenna at port-1 and port-2 for diode OFF and diode ON instances.

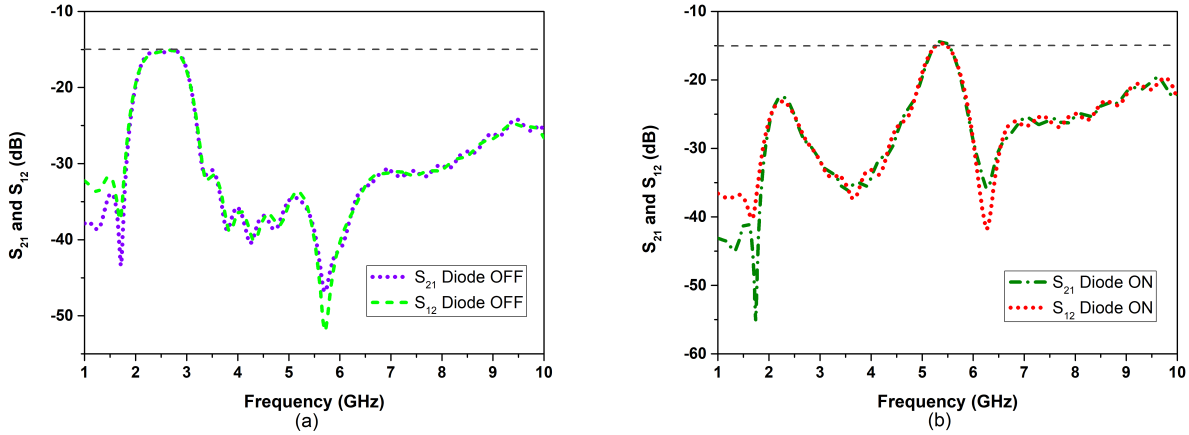

FIGURE 6. Simulation results of $|S_{21}|$ and $|S_{12}|$ of the frequency reconfigurable antenna (a) diode OFF (b) diode ON.

'd' on the rectangular slotted structure is shown in Fig. 4. It is to be noted from Fig. 4(a) and Fig. 4(b), the resonant frequency increases with increasing the parameter value 'f' (slot gap), whereas the resonant frequency decreases when increasing the parameter value 'd' (loop length). The antenna resonating at a fixed frequency of 2.17 GHz (at port-1) in the two cases diode OFF and diode ON. The magnitude of reflection coefficient $|S_{11}| < -25$ dB is achieved at port-1. Similarly, the resonance frequencies of 2.85 GHz and 5.52 GHz are obtained at port-2 for both diode OFF and diode ON cases, respectively. However, the magnitude of reflection coefficient $|S_{22}| < -15$ dB is achieved at port-2. Simulation results of reflection coefficient versus frequency of the frequency reconfigurable antenna at port-1 and port-2 for diode OFF and diode ON instances are shown in Fig. 5. The simulation results of transmission coefficients ($|S_{21}|$ and $|S_{12}|$) versus frequency for both the instances of diode OFF and diode ON are shown in Fig. 6. Good isolation of less than –18 dB is achieved between the two ports of the antenna from 1 GHz to 10 GHz. The isolation between these two ports is enhanced with the optimization of dimensions of open-loop slots corresponding to feed line sizes. The simulation results of surface current distributions of the antenna at port-1 (2.17 GHz) and port-2 (2.85 GHz and 5.52 GHz) for diode OFF and diode ON instances are shown in Fig. 7. It is observed that the high-density current distribution at the frequencies of respective ports and there is no such current on other frequencies of the ports. For example, the resonance frequency is similar for both diode cases at port-1 and the surface current is observed at that port related open-loop slot only. Similarly, the resonance frequency is changing from 2.85 GHz to 5.52 GHz at port-2 according to the placement of the diode on the corresponding open-loop slot. These simulation results reveal that the antenna shows frequency reconfiguration and independent frequency control simultaneously. Altering the port-1 rectangular open-loop slot dimensions does not affect the port-2 resonance frequency, and there is no variation in operating frequency at port-1 while changing the size of the C-shaped port-2 open-loop slot as well. Besides, a large frequency separation of greater than 2 GHz is achieved at port-2 during the frequency reconfiguration due to the insertion of the PIN diode on an open-loop slot. The antenna realized gains of 2.5 dB and 2.3/2.1 dB are obtained at resonance frequencies of 2.17 GHz

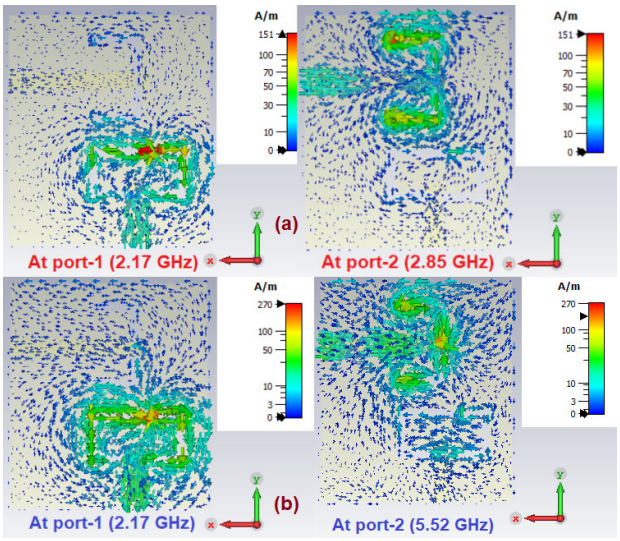

FIGURE 7. Surface current distributions of the frequency reconfigurable antenna (a) diode OFF (b) diode ON.

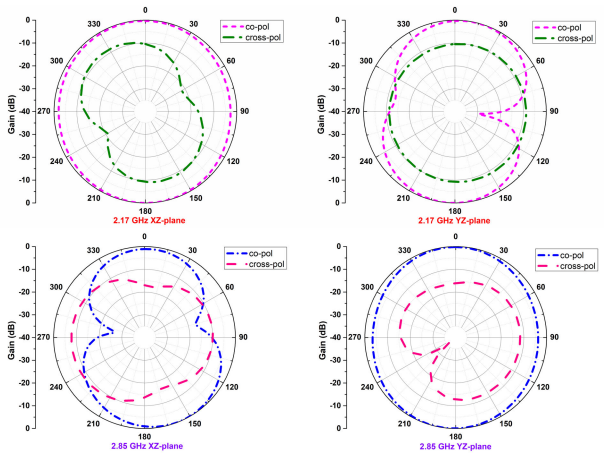

FIGURE 8. Simulation results of normalized radiation patterns of the frequency reconfigurable antenna when the diode is OFF (2.17 GHz at port-1 and 2.85 GHz at port-2).

and 2.85/5.52 GHz at their corresponding ports of port-1 and port-2, respectively. Further, the radiation characteristics of the antenna at their resonance frequencies are also discussed for the contexts of diode OFF and diode ON. The normalized simulation radiation patterns of the frequency reconfigurable antenna for the situation diode OFF at 2.17 GHz (port-1) and 2.85 GHz (port-2) are shown in Fig. 8. These radiation patterns are analyzed with the two principal planes of co-polarization ($\phi = 0^0$, XZ-plane) and cross-polarization ($\phi = 90^0$, YZ-plane) and it can be observed that all the patterns are directional with a cross-polarization gain of less than –15 dB. Similar radiation patterns are obtained with simulation cross-polarization gain of less than –10 dB for the case of diode ON and the corresponding patterns are shown in Fig. 9.

The frequency reconfigurable antenna is fabricated on a specified substrate using the S103 ProtoMat LPKF machine. The capacitor of 100 pF from Murata for DC blocking and

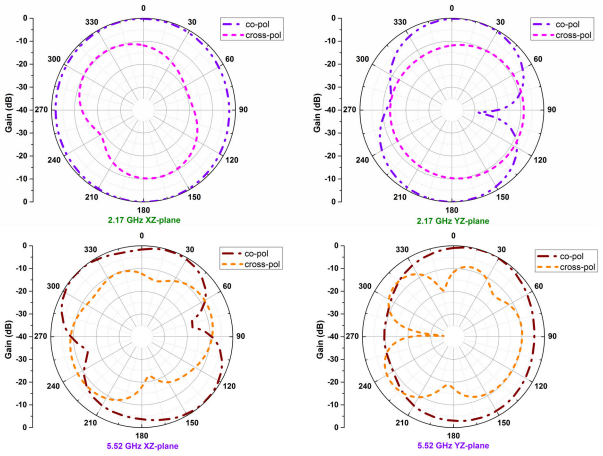

FIGURE 9. Simulation results of normalized radiation patterns of the frequency reconfigurable antenna when the diode is ON (2.17 GHz at port-1 and 5.52 GHz at port-2).

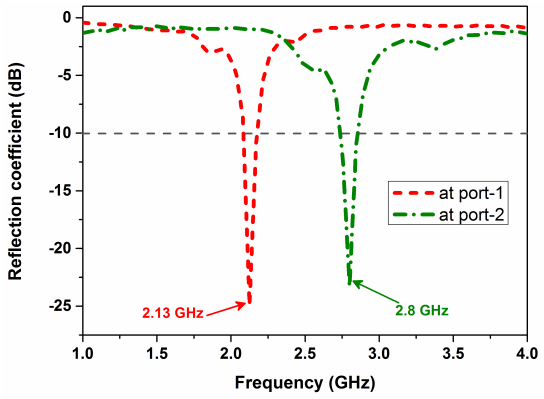

FIGURE 10. Measured reflection coefficients ($|S_{11}|$ and $|S_{22}|$) of the frequency reconfigurable antenna at port-1 and port-2.

PIN diode (BAR64-02V) from Infineon technologies for switching operation is chosen such that the electrical characteristics of the diode from datasheet are diode forward voltage drop (V_f)=0.67V, parallel resistance (R_p)=10KΩ, parallel capacitance (C_p)=0.17pF, series inductance (L_f)=1nH, and forward resistance (R_f)=2.1Ω. The PIN diode is soldered in a suitable position on the antenna ground plane. Similarly, the capacitor is positioned in a respective place on the open-ended slot. Two 50Ω SMA coaxial connectors are soldered on corresponding feed lines for the maximum RF power transmission. First, the antenna is measured for input reflection coefficients by connecting its two ports to the respective ports on the E8363C PNA network analyzer. The measured results of reflection coefficients of the proposed antenna at port-1 and port-2 are shown in Fig. 10. The transmission coefficients ($|S_{21}|$ and $|S_{12}|$) of the antenna are also measured and plotted in Fig. 11. Good isolation of less than –18 dB is achieved between the two ports. The antenna realized gains of 2.3 dB and 2.1 dB are measured at 2.13 GHz (port-1) and 2.8 GHz (port-2) frequencies using an antenna measurement system in the anechoic chamber. Further, the antenna radiation patterns are measured using a transmit antenna (horn),

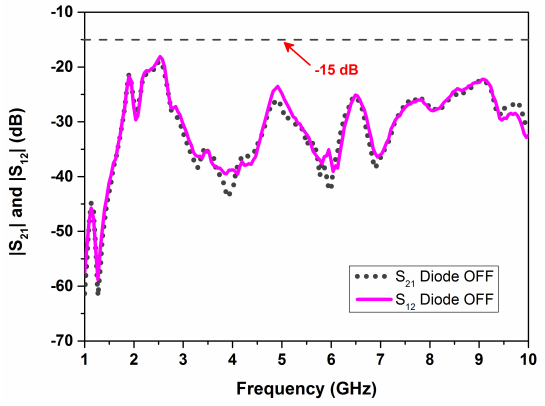

FIGURE 11. Measured transmission coefficients ($|S_{21}|$ and $|S_{12}|$) of the frequency reconfigurable antenna between port-1 and port-2.

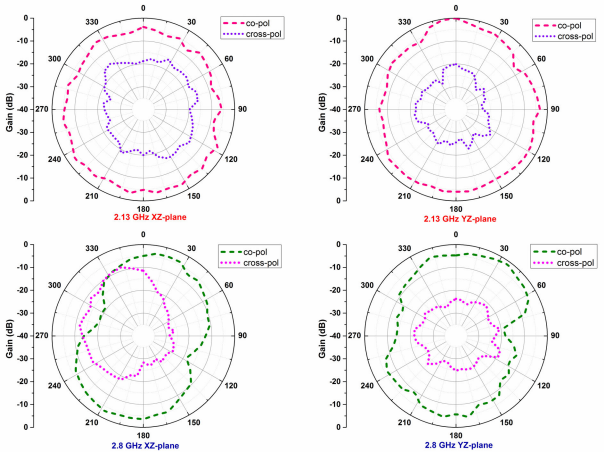

FIGURE 12. Measured results of normalized radiation patterns of the frequency reconfigurable antenna at 2.13 GHz (port-1) and 2.8 GHz (port-2).

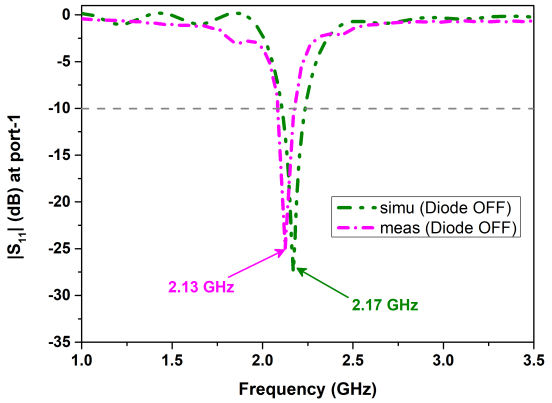

FIGURE 13. Simulation and measured results of reflection coefficient versus frequency when port-1 is excited.

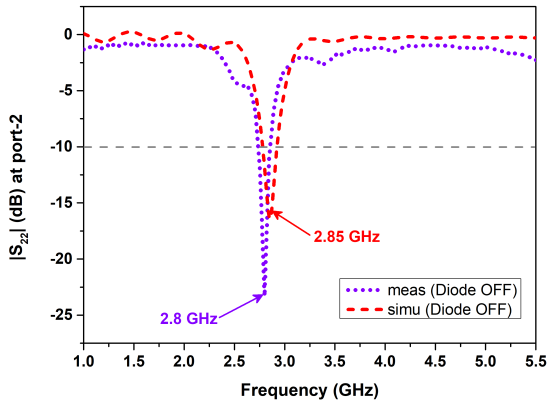

FIGURE 14. Simulation and measured results of reflection coefficient versus frequency when port-2 is excited.

varying the gain from 3 dB to 16 dB in a frequency range from 0.8 GHz to 18 GHz. The frequency reconfigurable antenna is placed on a chamber in receiving mode at a distance of greater than one meter (far-field distance) from the transmitting antenna. The measured results of normalized radiation patterns of the proposed antenna at two ports are shown in Fig. 12. It shows that the cross-polarization gain of less than –15 dB was obtained with bi-directional radiation patterns at 2.13 GHz and 2.8 GHz resonance frequencies. The simulation and measured results of reflection coefficient versus frequency of the antenna when port-1 is excited are shown in Fig. 13. The measured resonance frequency of 2.13 GHz is good matching with the simulation frequency of 2.17 GHz. The magnitude of measured $|S_{11}|< -20$ dB is achieved. The simulation and measured results of reflection coefficient versus frequency of the antenna when port-2 is excited are shown in Fig. 14. The measured resonance frequency of 2.8 GHz is well-matched with the simulation frequency of 2.85 GHz. The magnitude of measured $|S_{22}|< -20$ dB is obtained. The design details and result analysis of a rectifying circuit for the conversion of received RF power (at port-1) to desired DC control signal to turn ON the PIN diode at antenna port-2 have been discussed in the next subsection.

B. RECTIFYING CIRCUIT

The rectifying circuit is designed and fabricated on a 1.52 mm thickness Rogers 4003C substrate ($\epsilon_r = 3.3$ and $\tan\delta = 0.0027$). A single-stage Villard voltage doubler configuration is used for the design of a rectifier circuit comprising of the two Schottky diodes (SMS 7630-079LF), two capacitors (100 pF), one load resistor (2.2 KΩ), and transmission lines based stepped impedance matching network.

The rectifier circuit is simulated using Keysight Technologies ADS software to optimize voltage, reflection coefficient, and input impedance before the implementation of its final prototype. The Schottky diode is chosen with a low threshold voltage (V_{th}) of 147 mV [breakdown voltage (V_{br}) =2V, series resistance (R_s) = 20Ω, zero-bias junction capacitance (C_{j0}) = 0.14 pF] [31]. The schematic diagram of the rectifier circuit with an impedance matching network is shown in Fig. 15. The capacitor C_1 is placed before the diodes act as DC blocking component to stop the harmonics and protect the RF source/antenna. Similarly, the capacitor C_2 is positioned parallel to the load resistor acts as a DC pass filter, and it allows only DC signals. In the simulator, a microstrip

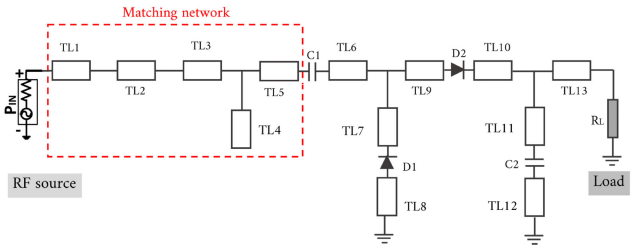

FIGURE 15. Schematic diagram of the rectifying circuit with an impedance matching network (TL1 = 3.4 mm/4.7 mm, TL2 = 10 mm/10 mm, TL3 = 4 mm/4.6 mm, TL4 = 1.5 mm/2 mm, TL5 = 1.6 mm/4 mm, TL6 = 3 mm/4.3 mm, TL7 = 3 mm/4.1 mm, TL8 = 3 mm/3.6 mm, TL9 = 3 mm/4.7 mm, TL10 = 3 mm/8.9 mm, TL11 = 3 mm/5.2 mm, TL12 = 3 mm/3.8 mm, TL13 = 3 mm/3.2 mm).

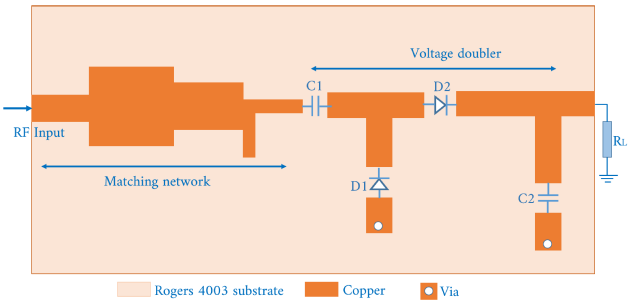

FIGURE 16. Final configuration of the rectifier circuit for fabrication.

T-junction is chosen to connect the main transmission lines in the rectifier for the optimization and generation of the equivalent layout before fabrication. The size of the rectifying circuit is $53 \times 21\ mm^2$. The final configuration of the rectifying circuit for fabrication on the specified substrate is shown in Fig. 16. The rectifier is designed to operate at a similar frequency of 2.1 GHz at port-1 of the frequency reconfigurable antenna. First, the reflection coefficient characteristics are primarily analyzed for different load resistances (0.5 KΩ to 4.5 KΩ) at 0 dBm input RF power, which results in a good impedance matching of less than –30 dB at 2.5 KΩ. As shown in Fig. 17(a), poor impedance matching is observed at lower and higher resistance values. After optimizing load resistance at 2.5 KΩ, the rectifier is further simulated for output DC voltage (V_0) versus load resistance (R_L) by varying the different input RF powers from –10 dBm to 10 dBm. From Fig. 18(a), the rectifier shows a maximum voltage of 1.9V at an input power of 10 dBm and load resistance of 2.5 KΩ. The voltage reached its maximum value and saturated beyond the optimized load resistance at an input power (P_{in}) of 10 dBm. The RF to DC conversion efficiency of the rectifier is computed using the below equation (1).

$$\text{Efficiency}(\%) = \frac{V_0^2/R_L}{P_{\text{in}}} \times 100 \tag{1}$$

where V_0 is output DC voltage obtained at the load resistor (R_L) and P_{in} is input power received from the RF source.

Fig. 18 (b) shows the peak RF to DC conversion efficiency of 59.8% is achieved at 2.1 GHz resonance frequency, 0 dBm input power, and the optimized load resistance of 2.5 KΩ. From these results, it can be concluded that the rectifier possesses a maximum efficiency at the optimized load resistance and an input RF power of 2.5 KΩ and 0 dBm, respectively. The efficiency results also reveal that the diode undergoes an early breakdown at an input power of greater than 0 dBm. That means the conversion efficiency drops to lower values while increasing the load resistance. The rectifier is simulated to further analyze the variation of output voltage versus input power at a fixed load resistance from 0.5 KΩ to 4.5 KΩ. Simulation results of output voltage versus input power of the rectifier circuit at different load resistances are shown in Fig. 19(a). In this plot, the rectifier reaches its maximum voltage value at specified input power and load resistance. Fig. 19(b) confirmed that the rectifier possesses a maximum efficiency of 59.8% at an input power of 0 dBm and load resistance of 2.5 KΩ. The experimental resistance value of 2.2 KΩ is finalized due to the unavailability of the exact resistance value of 2.5 KΩ. These values are kept fixed for the experimental analysis of the rectifier after fabrication. Simulation results of output voltage and efficiency versus resonance frequency (2.1 GHz) of the rectifier circuit at 0 dBm input power and finalized load resistance of 2.2 KΩ are shown in Fig. 20(a). The rectifier circuit shows a peak output voltage and efficiency at its resonance frequency of 2.1 GHz as well. To verify the experimental performance, the rectifier is initially measured for reflection coefficient and output DC voltage. The reflection coefficient is measured by integrating the network analyzer port directly into the rectifier. Simulation and measured results of $|S_{11}|$ versus frequency of the rectifier are shown in Fig. 17(b). The measured result is a good agreement with the simulation reflection coefficient. After this, the rectifier input port is connected to the signal generator output port for receiving the RF power. The output voltage is measured using a digital multimeter according to the finalized optimal input power value (0 dBm) and connected load resistance (2.2 KΩ). Simulation and measured output voltage and efficiency versus input power of the rectifier at 0 dBm input power and 2.2 KΩ load resistance are shown in Fig. 20(b). The measured RF to DC conversion efficiency of 54.9% is obtained at an input power of 0 dBm. The experimental analysis of the proposed antenna and autonomous switching of frequency bands have been discussed in the next section.

III. RESULTS AND DISCUSSION

To demonstrate the autonomous reconfigurability of the resonant frequency of the proposed antenna, port-1 of the antenna is used to receive the control signal which is transmitted from the control unit as an RF signal. Port-1 is connected to the rectifier circuit to convert the received RF signal to DC control voltage as shown in Fig. 21. The rectified signal is applied to the PIN diode which is used to reconfigure the resonant frequency of the proposed antenna at port 2. The antenna received powers are measured at different distances between transmit antenna (horn) and the proposed antenna by applying the fixed input power of 20 dBm. The output voltage

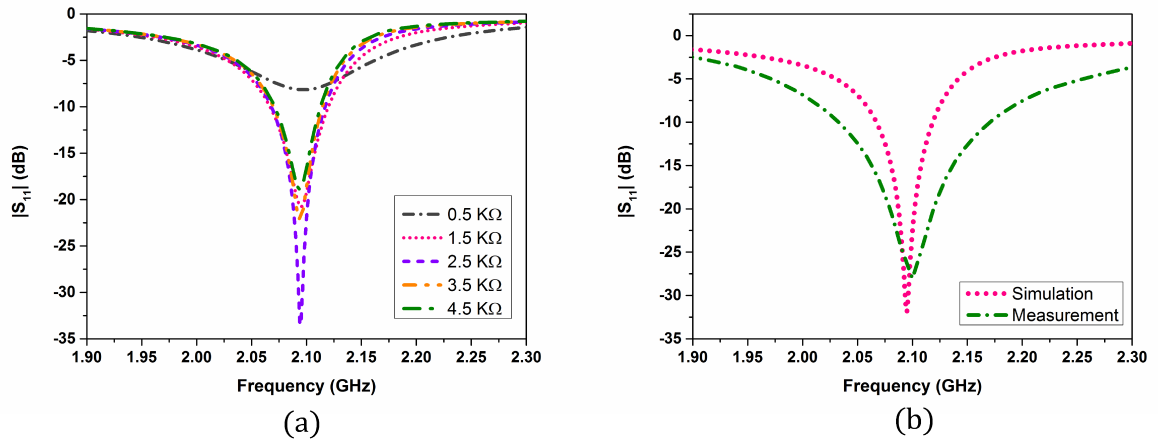

FIGURE 17. (a) Simulation results of $|S_{11}|$ versus frequency of the rectifier circuit at different load resistances. (b) Simulation and measured results of $|S_{11}|$ versus frequency of the rectifier circuit.

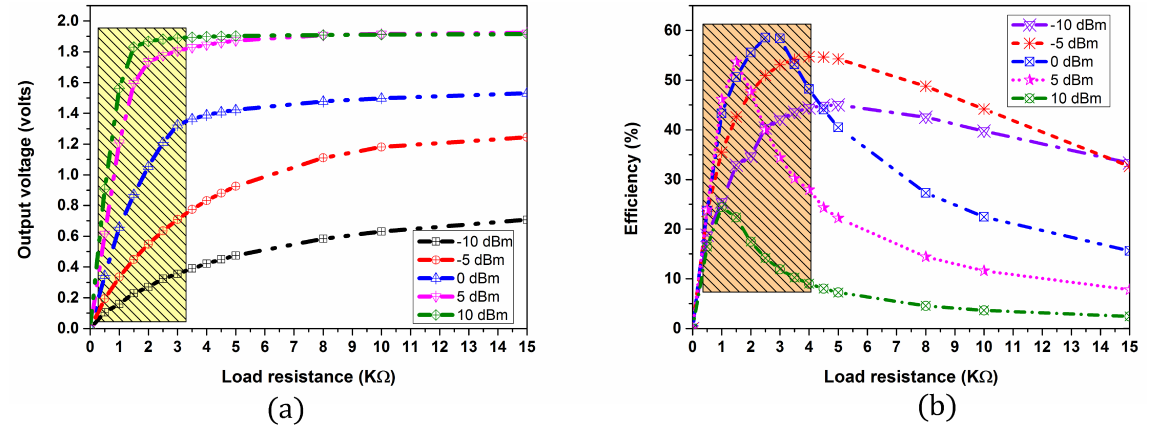

FIGURE 18. Simulation results of the rectifier circuit at different input powers (a) output voltage versus load resistance (b) efficiency versus load resistance.

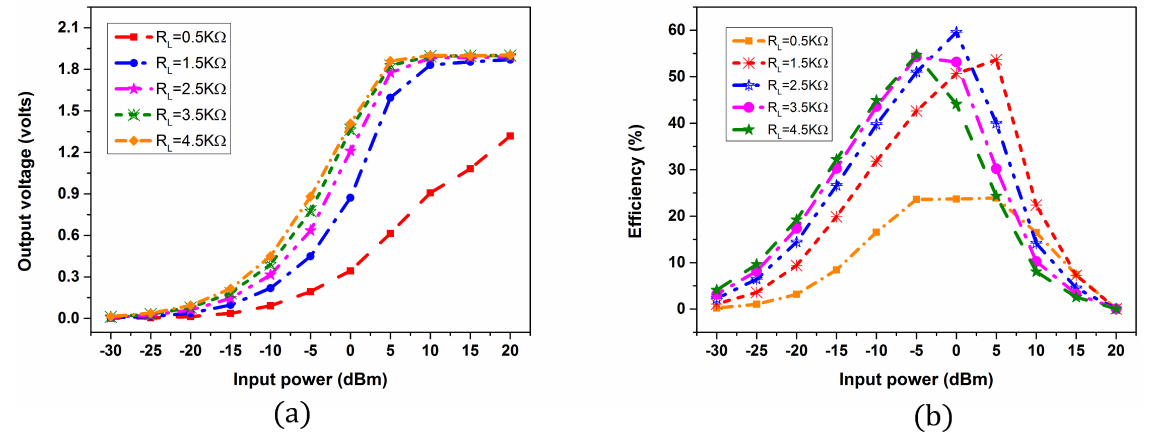

FIGURE 19. Simulation results of the rectifier circuit at different load resistances (a) output voltage versus input power (b) efficiency versus input power.

is measured at the load resistor using a digital multimeter. The RF to DC conversion efficiency is calculated using the above equation (1). The measured results of output voltage and calculated efficiency versus input power of the proposed autonomous frequency reconfigurable antenna are shown in Fig. 22. This figure shows that the measured output voltage

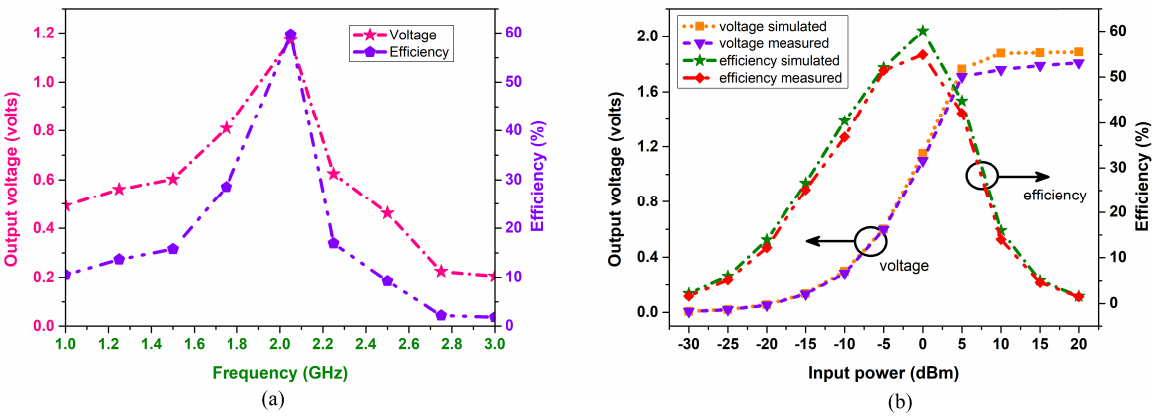

FIGURE 20. Results of the rectifier circuit at 0 dBm input power and 2.2 KΩ load resistance (a) simulated rectified output voltage and efficiency versus frequency (b) simulated and measured output voltage and efficiency versus input power.

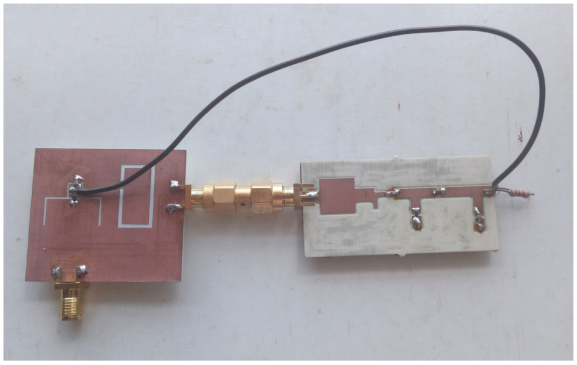

FIGURE 21. Fabrication prototype of the proposed autonomous frequency reconfigurable antenna.

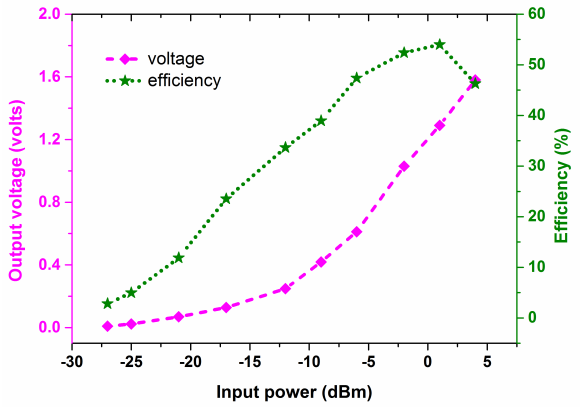

FIGURE 22. Measured results of output voltage and efficiency versus input power (antenna received power) of the autonomous frequency reconfigurable antenna at 2.1 GHz frequency and an optimized value of 2.2 KΩ load resistance.

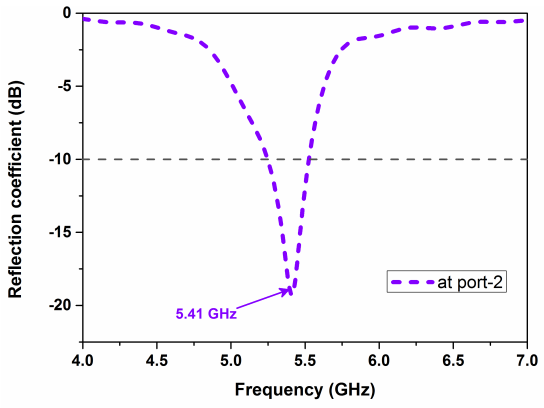

FIGURE 23. Measured result of reflection coefficient versus frequency of the proposed antenna at port-2 when the diode is ON.

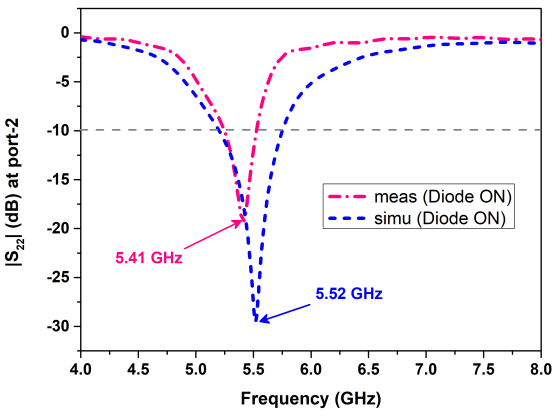

FIGURE 24. Simulation and measured results of reflection coefficient versus frequency of the proposed antenna at port-2 when the diode is ON.

and conversion efficiency of 1.29V and 53.8% at an input power (antenna received power) of 0.9 dBm, respectively.

To observe the autonomous frequency switching, the proposed antenna is excited with the transmitting (horn) antenna and connects its port-2 (proposed antenna) to the network analyzer. In this measurement we have observed that the frequency is adaptively switched from 2.8 GHz (Diode OFF) to 5.41 GHz (Diode ON) at the input power (antenna received power) of −2 dBm at port-2. The proposed antenna effectively converted the required DC control voltage of 0.67V at this input power for the actuation of the PIN diode at port-2. The measured result of reflection coefficient versus

TABLE 1. Performance comparison of the proposed antenna with recently reported similar kind of antennas.

Ref.	Antenna type	Operating frequency	Size (mm^2)	Size (λ^2)	No. of elements used	Circuit complexity	No. of diodes used	No. of ports
[7]	Composite right/left	0.67, 1.04, 2.24	56×55	0.125×0.122	1	Less	1	1
[10]	Bow-tie microstrip	2.02, 2.19, 2.37	49.4×47.2	0.332×0.317	6	Medium	2	1
[21]	Monopole	0.76, 1.87	280×280	0.709×0.709	12	Medium	8	1
[25]	Asymmetric CPW fed	2.4, 3.8, 5.6	24×19	0.192×0.152	6	Less	2	1
[26]	Monopole	0.43 – 1	60×100	0.086×0.143	10	High	1	1
[27]	SIW	2.4, 5.7	53.5×53.5	0.428×0.428	12	Medium	12	1
[28]	Microstrip patch	1.23, 1.57	215×190	0.881×0.779	14	High	9	1
[32]	Dual-T-shaped monopole	5.2, 5.8	87×91	1.508×1.577	3	Less	1	1
[33]	Microstrip patch	2.45, 5.8	52×19	0.427×0.153	5	High	1	1
This work	Dual-port slot	2.13, 2.8/5.41	120×35	0.852×0.248	5	Less	1	2

where 'λ' is free space wavelength at lower band frequency of the corresponding antenna.

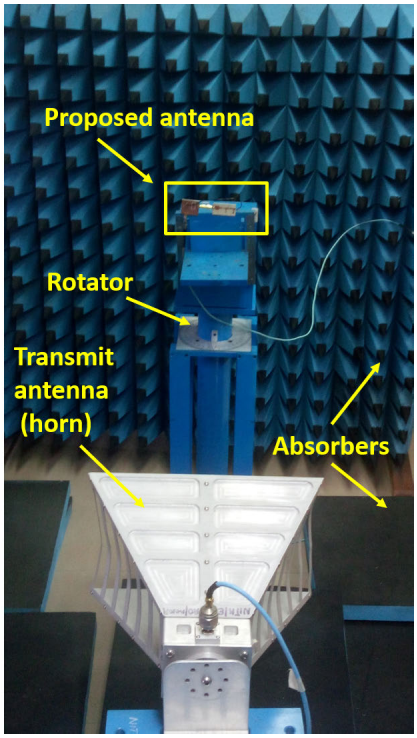

FIGURE 25. Photograph of the proposed antenna is mounted in a chamber in receiving mode for the measurement of switchable frequency at port-2 when the diode is ON.

frequency of the proposed antenna at port-2 when the diode is ON is shown in Fig. 23. This measured result has also been compared with the corresponding simulation result. The simulation and measured results of reflection coefficient versus frequency of the proposed antenna at port-2 when the diode is ON are shown in Fig. 24. The measured result is slightly shifted to the lower frequency side from the simulation result of 5.52 GHz and resonating at a frequency of 5.41 GHz. The magnitude of measured $|S_{22}|< -15$ dB is obtained. The photograph of the proposed antenna is mounted in the anechoic chamber in receiving mode for the measurement of switchable frequency at port-2 when the diode is ON is shown in Fig. 25. The proposed antenna is compared with the previously reported antennas in the literature in terms of no. of elements used, circuit complexity, no. of diodes, and no. of ports. Comparison of the proposed autonomous frequency reconfigurable antenna with recently reported similar kind of antennas is listed in Table 1. Recently, a self-biased adaptive reconfigurable rectenna and frequency-reconfigurable rectenna with an adaptive matching stub are reported in [32], [33] for microwave power transmission. In [32], the impedance matching stub is adaptively connected to and disconnected from the rectifier circuit when the transistor switch is ON/OFF depends on rectifier output DC voltage. Similarly, the rectifier proposed in [33] utilized its rectified DC voltage supply to a PIN diode for adaptive frequency reconfiguration. These works are mainly focused on frequency reconfiguration on the rectifier side but in our proposed work autonomous frequency reconfiguration occurs due to rectified DC voltage is directly connected to the PIN diode on the antenna. The reconfigurable antennas mentioned in the reference list except [28] are switchable at different frequencies using an external DC bias voltage. Compared to these antennas, the proposed antenna can be automatically frequency switching at port-2 without the need for an external DC control signal with an additional biasing circuit and does not disturb the existing resonance frequency at port-1. The microstrip patch reconfigurable antenna in [28] is switchable automatically by connecting the power splitter and bandpass filter in between the antenna and rectifying circuit. This configuration makes the overall antenna structure complex and inconvenient for integrating other microwave devices. In addition to this, the switchable frequency separation is 0.34 GHz (1.23 GHz to 1.57 GHz) only. In our proposed work, a novel dual-port frequency reconfigurable antenna and rectifying circuit are only used for autonomous frequency switching. However, the experimental results show that the proposed antenna is effectively switching from 2.8 GHz to 5.41 GHz with an impedance matching ($|S_{11}|$) of less than –18 dB. The change of batteries for continuous DC supply to the low-power electronic devices (PIN/Varactor diodes) in remote locations is difficult. The autonomous frequency reconfigurable antennas provide continuous DC supply to the low-power electronic devices for adaptive switching of frequency bands. The reason for proposing the two ports in our topology is port-1 is useful for the generation of the required control signal (DC voltage) to actuate the PIN

diode by using RF to DC conversion circuit, and port-2 is for transmit/receive RF power. In our design, the antenna port-1 frequency does not change when port-2 is excited at two operating frequencies. However, the autonomous frequency reconfigurable antenna proposed in our work is found to be suitable for microwave energy harvesting (through port-1) and data communication (through port-2). The proposed antenna design has an advantage in terms of low-cost, easy fabrication, compact design, flexible structure, and simplicity.

IV. CONCLUSION

In this article, an autonomous frequency reconfigurable antenna using slotline open-loop resonators has been demonstrated for autonomous switching of frequency bands. For this, a low threshold voltage PIN diode that acts as a switch is placed on the corresponding open-loop slot of the antenna and actuated with the efficient rectifying circuit operating at the most functional UMTS band of 2.1 GHz. The two-channel frequency reconfiguration with independent control is observed in both simulation and experimental results as well. The control of diode ON or OFF is mainly dependent on the antenna's received power and rectifying circuit output DC voltage. Besides, the isolation and coupling between the two ports are good at the operating frequencies. With the expansion of reconfiguration technology, the proposed autonomous frequency reconfigurable antenna can be used to provide the required DC voltage to low-power devices for adaptive frequency switching applications.

REFERENCES

[1] H. Boudaghi, M. Azarmanesh, and M. Mehranpour, "A frequency-reconfigurable monopole antenna using switchable slotted ground structure," *IEEE Antennas Wireless Propag. Lett.*, vol. 11, pp. 655–658, Jun. 2012.

[2] G. Chen, X.-l. Yang, and Y. Wang, "Dual-band frequency-reconfigurable folded slot antenna for wireless communications," *IEEE Antennas Wireless Propag. Lett.*, vol. 11, pp. 1386–1389, Nov. 2012.

[3] M. Borhani, P. Rezaei, and A. Valizade, "Design of a reconfigurable miniaturized microstrip antenna for switchable multiband systems," *IEEE Antennas Wireless Propag. Lett.*, vol. 15, pp. 822–825, Nov. 2016.

[4] D. E. Anagnostou and A. A. Gheethan, "A coplanar reconfigurable folded slot antenna without bias network for WLAN applications," *IEEE Antennas Wireless Propag. Lett.*, vol. 8, pp. 1057–1060, Sep. 2009.

[5] C. Hung and T. Chiu, "Dual-band reconfigurable antenna design using slot-line with branch edge," *IEEE Trans. Antennas Propag.*, vol. 63, no. 2, pp. 508–516, Feb. 2015.

[6] A. Shahgholi, G. Moradi, and A. Abdipour, "Low-profile frequency-reconfigurable LTE-CRLH antenna for smartphones," *IEEE Access*, vol. 8, pp. 26487–26494, Feb. 2020.

[7] X. Yang, J. Xiao, J. Wang, and L. Sheng, "Compact frequency reconfigurable antennas based on composite right/left-handed transmission line," *IEEE Access*, vol. 7, pp. 131663–131671, Sep. 2019.

[8] L. Han, C. Wang, X. Chen, and W. Zhang, "Compact frequency-reconfigurable slot antenna for wireless applications," *IEEE Antennas Wireless Propag. Lett.*, vol. 15, pp. 1795–1798, Mar. 2016.

[9] H. B. Kim and K. C. Hwang, "Dual-port spidron fractal slot antenna for multiband gap-filler applications," *IEEE Trans. Antennas Propag.*, vol. 60, no. 10, pp. 4940–4943, Oct. 2012.

[10] D. Behera, B. Dwivedy, D. Mishra, and S. K. Behera, "Design of a CPW fed compact bow-tie microstrip antenna with versatile frequency tunability," *IET Microw., Antennas Propag.*, vol. 12, no. 6, pp. 841–849, Apr. 2018.

[11] T. Li, H. Zhai, X. Wang, L. Li, and C. Liang, "Frequency-reconfigurable bow-tie antenna for Bluetooth, WiMAX, and WLAN applications," *IEEE Antennas Wireless Propag. Lett.*, vol. 14, pp. 171–174, Feb. 2015.

[12] Y. Cai, Y. J. Guo, and A. R. Weily, "A frequency-reconfigurable quasi-Yagi dipole antenna," *IEEE Antennas Wireless Propag. Lett.*, vol. 9, pp. 883–886, Sep. 2010.

[13] P.-Y. Qin, A. R. Weily, Y. J. Guo, T. S. Bird, and C.-H. Liang, "Frequency reconfigurable quasi-Yagi folded dipole antenna," *IEEE Trans. Antennas Propag.*, vol. 58, no. 8, pp. 2742–2747, Aug. 2010.

[14] A. Bhattacharjee and S. Dwari, "Wideband frequency reconfigurable patch antenna for various wireless applications," in *Proc. IEEE Indian Conf. Antennas Propogation (InCAP)*, Dec. 2018, pp. 1–4.

[15] Y. Wang, Y. Liu, H. Du, C. Liu, Q. Xue, X. Gao, S. Li, and Y. Lu, "A frequency reconfigurable microstrip antenna based on (Ba, Sr)TiO_3 substrate," *IEEE Trans. Antennas Propag.*, vol. 63, no. 2, pp. 770–775, Feb. 2015.

[16] A. Khidre, F. Yang, and A. Z. Elsherbeni, "A patch antenna with a varactor-loaded slot for reconfigurable dual-band operation," *IEEE Trans. Antennas Propag.*, vol. 63, no. 2, pp. 755–760, Feb. 2015.

[17] C.-Y.-D. Sim, T.-Y. Han, and Y.-J. Liao, "A frequency reconfigurable half annular ring slot antenna design," *IEEE Trans. Antennas Propag.*, vol. 62, no. 6, pp. 3428–3431, Jun. 2014.

[18] H. Mirzaei and G. V. Eleftheriades, "A compact frequency-reconfigurable metamaterial-inspired antenna," *IEEE Antennas Wireless Propag. Lett.*, vol. 10, pp. 1154–1157, Oct. 2011.

[19] H. Li, J. Xiong, Y. Yu, and S. He, "A simple compact reconfigurable slot antenna with a very wide tuning range," *IEEE Trans. Antennas Propag.*, vol. 58, no. 11, pp. 3725–3728, Nov. 2010.

[20] S. W. Lee and Y. Sung, "Compact frequency reconfigurable antenna for LTE/WWAN mobile handset applications," *IEEE Trans. Antennas Propag.*, vol. 63, no. 10, pp. 4572–4577, Oct. 2015.

[21] N. Nguyen-Trong, A. Piotrowski, and C. Fumeaux, "A frequency-reconfigurable dual-band low-profile monopolar antenna," *IEEE Trans. Antennas Propag.*, vol. 65, no. 7, pp. 3336–3343, Jul. 2017.

[22] M. Sun, Z. Zhang, F. Zhang, and A. Chen, "L/S multiband frequency-reconfigurable antenna for satellite applications," *IEEE Antennas Wireless Propag. Lett.*, vol. 18, no. 12, pp. 2617–2621, Dec. 2019.

[23] Y. Tawk, "Physically controlled CubeSat antennas with an adaptive frequency operation," *IEEE Antennas Wireless Propag. Lett.*, vol. 18, no. 9, pp. 1892–1896, Sep. 2019.

[24] S. Subbaraj, M. Kanagasabai, M. G. N. Alsath, S. K. Palaniswamy, S. Kingsly, I. Kulandhaisamy, A. K. Shrivastav, R. Natarajan, and S. Meiyalagan, "A compact frequency-reconfigurable antenna with independent tuning for hand-held wireless devices," *IEEE Trans. Antennas Propag.*, vol. 68, no. 2, pp. 1151–1154, Feb. 2020.

[25] K. Sreelakshmi, G. S. Rao, and M. N. V. S. S. Kumar, "A compact grounded asymmetric coplanar strip-fed flexible multiband reconfigurable antenna for wireless applications," *IEEE Access*, vol. 8, pp. 194497–194507, Nov. 2020.

[26] A. Kantemur, J. Tak, P. Siyari, A. H. Abdelrahman, M. Krunz, and H. Xin, "A novel compact reconfigurable broadband antenna for cognitive radio applications," *IEEE Trans. Antennas Propag.*, vol. 68, no. 9, pp. 6538–6547, Sep. 2020.

[27] J. Qin, X. Fu, M. Sun, Q. Ren, and A. Chen, "Frequency reconfigurable antenna based on substrate integrated waveguide for S-band and C-band applications," *IEEE Access*, vol. 9, pp. 2839–2845, Jan. 2021.

[28] L. Hinsz and B. D. Braaten, "A frequency reconfigurable transmitter antenna with autonomous switching capabilities," *IEEE Trans. Antennas Propag.*, vol. 62, no. 7, pp. 3809–3813, Jul. 2014.

[29] H. Liu, L. Shen, L. Y. Shi, Y. Jiang, X. Guan, and T. Wu, "Dual-mode dual-band bandpass filters design using open-loop slotline resonators," *IET Microw., Antennas Propag.*, vol. 7, no. 12, pp. 1027–1034, Sep. 2013.

[30] J.-S. Hong and M. J. Lancaster, "Couplings of microstrip square open-loop resonators for cross-coupled planar microwave filters," *IEEE Trans. Microw. Theory Techn.*, vol. 44, no. 11, pp. 2099–2109, Dec. 1996.

[31] Skyworks. [Online]. Available: http://www.skyworksinc.com

[32] P. Lu, K. M. Huang, Y. Yang, F. Cheng, and L. Wu, "Frequency-reconfigurable rectenna with an adaptive matching stub for microwave power transmission," *IEEE Antennas Wireless Propag. Lett.*, vol. 18, no. 5, pp. 956–960, May 2019.

[33] P. Lu, C. Song, F. Cheng, B. Zhang, and K. Huang, "A self-biased adaptive reconfigurable rectenna for microwave power transmission," *IEEE Trans. Power Electron.*, vol. 35, no. 8, pp. 7749–7754, Aug. 2020.

GERIKI POLAIAH (Student Member, IEEE) received the B.Sc. and M.Sc. degrees in physics from Sri Venkateswara University, Tirupati, India, in 2005 and 2007, respectively, and the M.Tech. degree in electronics and communication engineering from Jawaharlal Nehru Technological University Anantapur, India, in 2010. He is currently pursuing the Ph.D. degree in electronics and communication engineering with the National Institute of Technology Karnataka, Surathkal, India.

He has eight years of teaching experience, and his current research interests include rectifier integrated antennas, rectifying circuits, metasurfaces, and metamaterial-based antennas for wireless power transfer and energy harvesting applications.

KRISHNAMOORTHY KANDASAMY (Member, IEEE) received the B.E. degree in electronics and communication engineering from Bharathiar University, Coimbatore, in 2002, and the M.E. degree in communication systems from Anna University, Chennai, in 2007, and the Ph.D. degree in electrical engineering from the Indian Institute of Technology Bombay, Mumbai, in 2016.

He worked as a Member of Technical Staff at HCL Technologies Ltd., Bengaluru, and as a Deputy Engineer at Bharat Electronics, Bengaluru. He is currently an Assistant Professor with the Department of Electronics and Communication Engineering, National Institute of Technology Karnataka, Surathkal, India. He has published more than 60 research articles in international/national journals and conferences. He is involved in the design and fabrication of various microwave antennas and metasurfaces. His research interests include reconfigurable and multiband antenna design, metamaterials, anisotropic metasurfaces, and RF circuits for the next generation wireless communication systems.

MURALIDHAR KULKARNI (Senior Member, IEEE) received the B.E. degree in electronics engineering from the University Visvesvaraya College of Engineering, Bengaluru, in 1980, and the M.Tech. degree in satellite communication and remote sensing from the Indian Institute of Technology Kharagpur, in 1984, and the Ph.D. degree in electronics and communication engineering from JMI Central University, New Delhi, in 2006.

He worked as a Scientist at Central Power Research Institute, Bengaluru, and as an Aeronautical Engineer at Hindustan Aeronautics Ltd., Bengaluru. He served as an Assistant Professor with the Department of Electronics and Communication Engineering, University Visvesvaraya College of Engineering, and as an Associate Professor with the Department of Electronics and Communication Engineering, Delhi Technological University, New Delhi. Then, he joined the Department of Electronics and Communication Engineering, National Institute of Technology Karnataka (NITK), Surathkal, as a Faculty, in 2008, where he is currently a Full Professor in electronics and communication engineering. He has served as the HoD of ECE Department and as the Chairman of the Career Development Center, and a member of Board of Governors. He is currently a Coordinator of the Center of Excellence (CoE) in Wireless Sensor Networks, NITK. He has published more than 80 research articles in international/national journals and conferences. He has also authored/coauthored five very popular textbooks in the areas of microwaves and radars, digital signal processing, information theory and coding, and analog and digital communications. His current research interests include digital communications and networks (OFDM, WSN, SDN, congestion control, 5G networks, and the IoT), optical communications and networks (FSO), microwaves, and antenna systems.

Dr. Kulkarni is a fellow of IETE and a Life Member of ISTE and CSI. He has credited with several funded research projects and delivered keynote addresses/technical talks in international conferences and workshops.